SHAKE TABLE TESTS ON REINFORCED CONCRETE SHORT COLUMNS FAILING IN SHEAR

C.L. Wu[1], R.S. Su[2], S.J. Hwang[3] and Y.S. Yang[1]

[1] *Associate Research Fellow, Center for Research on Earthquake Engineering (NCREE), Taipei, Chinese Taiwan*
[2] *Former Graduate Student, Taiwan University of Science and Technology, Taipei, Chinese Taiwan*
[3] *Professor, Dept. of Civil Engineering, Taiwan University, Taipei, Chinese Taiwan*
Email: clwu@ncree.org.tw, sjhwang@ntu.edu.tw, ysyang@ncree.org.tw

ABSTRACT :

RC short columns are prone to pure shear failure due to insufficient transverse reinforcement, but there has been very limited research found in the literature on pure shear failure of short columns. As such, this study conducted shaking table tests on 4 specimen frames to investigate full-range structural behavior of RC short columns until complete collapse. A 10% low axial load was applied using lead packets, and ground motion record TCU082ew from the 1999 Chi-Chi earthquake was employed to excite the specimen frames. Through comparison with its companion full-scale cyclic test results, this study finds that shear strengths of short columns from dynamic tests are higher than those from cyclic tests. The existing predictive models are inclined to underestimate shear strengths of short columns, which is especially true for columns with nonductile detailing. In addition, the backbone model of ASCE/SEI 41-06 update for short columns also proves conservative.

KEYWORDS: Shaking table, dynamic collapse, RC short column, shear failure

1. INTRODUCTION

During the 1999 Chi-Chi earthquake, lots of short columns close to window sills in older school buildings failed in an unfavorable pure shear mode due to insufficient transverse reinforcement. The failure of RC columns can be categorized into 3 major mechanisms, pure flexure, flexure-shear and pure shear failure. There have been a number of laboratory tests on RC columns that are prone to fail in pure flexure and flexure-shear modes; however, there are few test results reported on pure shear failure, especially under realistic earthquake motions. In view that knowledge on the load deformation response of older RC short columns, especially post-peak behavior, is very limited in engineering and research community worldwide, this study aims to improve the understanding on full-range structural behavior by conducting laboratory tests on physical models and conducting simplified analyses on the observed results. Currently available assessment tools in existing design documents and research literature are carefully reviewed and hopefully the accuracy in predicting shear strength and drift capacity can be improved in the subsequent studies through the collected experimental database. In addition to shaking table tests on dynamic collapse of 1/2-scale specimen columns, there was another companion test program on full-scale isolated columns of identical design but subjected to quasi-static reversed cyclic loading under double curvature deformation. This arrangement allows for expanded database to facilitate comparison of experimental results from static and dynamic tests and the development of chart-based (e.g., ASCE/SEI 41-06), probability-based (e.g., Zhu et al. 2007) and mechanics-based drift capacity prediction models.

2. DESIGN OF SHAKING TABLE TESTS

Primary test variables studied herein were aspect ratio and seismic detailing (Table 1). A total of four half-scaled planar frames were tested, among which, three specimen frames were comprised of two identical short columns each (Fig. 1), and the fourth specimen frame was comprised of three short columns, with a center nonductile column and two outside flexural columns. The flexural columns were added to the specimen frame to partially simulate the gradual lateral and vertical failure mechanism that would be anticipated in a typical building during an earthquake. The authors believe that the study of load redistribution during structural collapse is of significant engineering interest, and through such three-column frame tests, it was confirmed that such phenomenon did exist, in particular vertical load redistribution.

Table 1 Configuration and reinforcement details of column specimens.

Column Code	4DL	4NL	3DL	3NL
Aspect Ratio	1:4	1:4	1:3	1:3
Detailing	Ductile	Nonductile	Ductile	Nonductile
Transverse Ties	D4@5cm	D4@15cm	D4@5cm	D4@15cm
	135° hook cross ties	90° hook	135° hook Cross ties	90° hook
Longitudinal Rebars	8 #4	16 #4	16 #4	16 #4
Cross Sectional Dimension	25*25cm	25*25cm	25*25cm	25*25cm
Clear Column Height (cm)	100	100	75	75

As a total, nine single RC column specimens were constructed, with footings cast first and then columns and column caps. After the column specimens were constructed, wet curing was continued for another two weeks. Standard concrete cylinders (15cm diameter by 30cm high) were cast at the same time as each concrete pour, and then cured under the same condition and in the same location as the column specimens. Compressive strength tests of three concrete cylinders were conducted at the test dates. The average concrete compressive strength for the columns and caps was 29.9MPa with 4.3% coefficient of variation, and was 42.1MPa for the footings (COV=5.5%). Average yield tensile strengths of the #4 longitudinal bars and D4 smooth steel wires for transverse reinforcement were 436MPa and 643MPa, respectively. The D4 steel wires were made through a cold-rolling operation of wires with a slightly larger diameter, with a consequence of an increase in its yield strength and a significant decrease in ductility since heat treatment (annealing) was not performed.

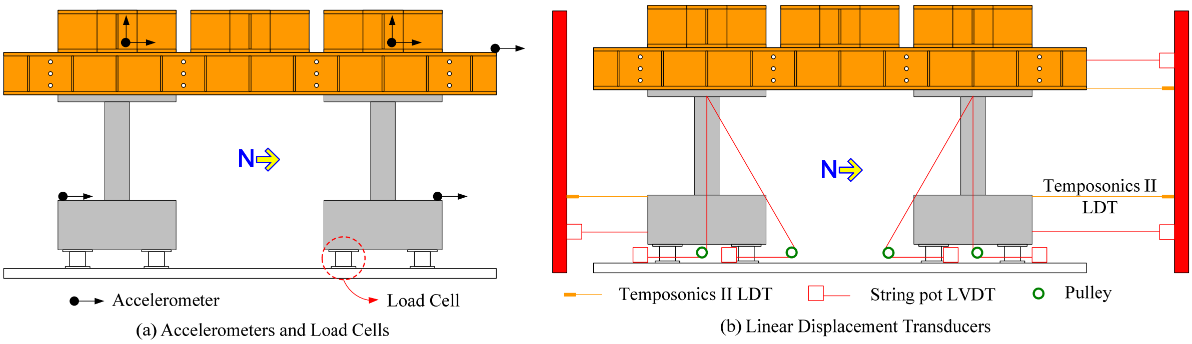

Figure 1 Location of load cells, accelerometers, and linear displacement transducers.

These columns can be categorized into 4 different types, listed as 4DL, 4NL, 3DL, and 3NL in Table 1, in which their dimensions and reinforcement information are also provided. As shown in Fig. 1, each frame consisted of two (or, three) concrete columns interconnected at the top by a fairly stiff mega beam made of A572 Grade 50 steel. Two load cells were installed beneath each of the footings. Lead packets were then mounted to the mega steel beam to achieve approximately $P/(A_g f_c')$ = 0.1 to each column (P = column axial load; A_g = gross cross sectional area of the column; f'_c = concrete compressive strength at the test date.)

Fig. 1 also shows the experimental setup of the specimen frame on the shaking table. The experimental setup aims for instrumented observation of global dynamic collapse of the columns. Load cells, accelerometers, Temposonics II and string pot linear displacement transducers (LDTs), strain gauges, and a digital image-based displacement measurement system were employed to collect experimental data of engineering interest. Strain gauges were attached to the surface of longitudinal and transverse reinforcing bars when construction was in progress; their locations were within zones where damage was expected to take place during simulated earthquake loadings. Accelerometers measured lateral and vertical accelerations at specified locations (Fig. 1a). Load cells were used to record column axial loads and shear forces during the shaking table tests. Column shear force is the lateral force measured by load cells installed beneath the footings minus the inertia force induced from the footing. Column axial load is the vertical force measured by load cells minus the footing weight. A positive value of axial load indicates compression. Bending moment at the column base is determined using a free-body equilibrium of the footing, including the shear and axial force outputs from load cells.

The base-shear response of the frame can be obtained either from accelerometers installed on the mass at the top of the frame or from load cells installed underneath the footings of columns. These data are compared in Fig. 2 to ensure the functionality of frictionless sliders installed on the steel supporting frame. These two curves have good agreement up to frame collapse.

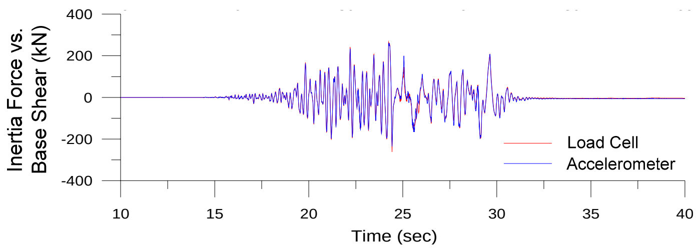

Figure 2 Comparison of base shear time histories of the frame obtained from accelerometers and load cells of Frame 3 (Test Run 4).

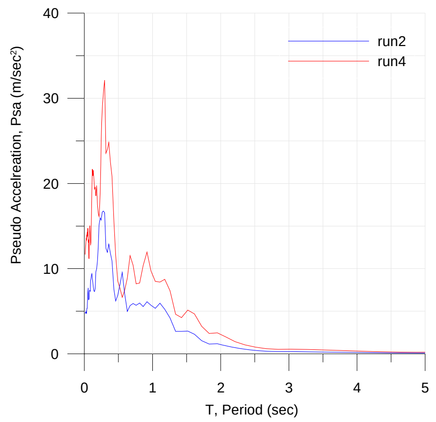

Figure 3 Response spectra of recorded table motions applied to Frame 3.

Table 2 Natural periods and viscous damping ratios of the virgin frames.

Frame No.	No. of Columns	Column Composition	Natural Period (sec)	Damping Ratio (%)
1	3	4DL + 4NL + 4DL	0.13	4.5
2	2	3DL + 3DL	0.10	4.2
3	2	3NL + 3NL	0.10	4.3
4	2	4NL + 4NL	0.10	3.6

Prior to the earthquake simulation tests, the test frames were subjected to low level (30cm/sec^2) white noise excitation. The natural periods and viscous damping ratios of the virgin frames were then identified using a transfer function between the top and base of the test frame, and results are reported in Table 2.

In the earthquake simulation tests, the EW component of the TCU082 accelerogram from the 1999 Chi-Chi Taiwan earthquake was employed as the input motion. Station TCU082 (24.148˚N latitude, 120.676˚E longitude) was 4.47 km from the surface rupture of Chelungpu fault, and recorded a peak ground acceleration (PGA) of 221.16cm/sec^2 in the EW direction. Station TCU082 was located in central Taiwan. Because a 1:2 geometric scale factor was applied to the test specimen, input ground motions were adjusted using a time compression factor of $1/\sqrt{2}$, which induced a higher strain rate than real earthquakes. The selected ground motion was modified with a trapezoidal frequency domain filter from 0.2Hz to 20Hz, and scaled to different PGA levels ranging from 0.4g to 1.5g until global collapse had been observed. Sample response spectra of the recorded table motions are presented in Fig. 3.

3. TEST OBSERVATIONS

Columns sustained pure shear failure as expected. Primary diagonal crack was observed at an inclination angle of approximately 60˚ to the horizontal in all cases (Fig. 4). Damage snapshots also suggest axial shortening of the columns due to sliding on the shear failure plane and crushing of the core concrete.

Frame 1 Center Column | Frame 2 South Column | Frame 3 South Column | Frame 4 South Column

Figure 4. Snapshots of column shear damage during the tests.

The 3-column frame allowed for observations of load redistribution, local collapse of the center column, and complete collapse of the whole frame. After the center nonductile column of the 3-column frame sustained severe shear damage, the axial load of this column was successfully redirected to outer ductile columns in a dramatic manner as shown in Fig. 5. Even though the total vertical load carrying capability of Frame 1 was kept mainly unchanged during the test, there was abrupt loss of vertical load carrying capacity in the center nonductile column and vertical load was redistributed to outer ductile columns. On the other hand, the 2-column frames allowed no load redistribution as they were composed of 2 identical columns. As shown in Fig. 6, there was no alternative path for load redistribution such that the vertical load carrying capacity dropped substantially. The drop of the total column axial force resulted from increase of the vertical inertia force of the mega steel beam and lead packets, while the increased vertical inertia force was induced from the dramatic loss of column's vertical load carrying capacity, sliding of along column's shear failure plane, and subsequent crushing of core concrete of columns. The loading mechanism of 2-column frames is very similar to the cyclic test of a single column except for the strain rate and input loading history. It is mentioned that these columns were also built in full-scale and each column was tested under a cyclic loading pattern in a companion project to facilitate comparison of experimental results between static and dynamic tests.

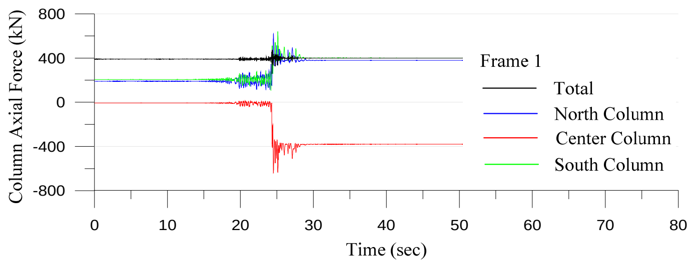

Figure 5. Vertical load redistribution of Frame 1 during the tests.

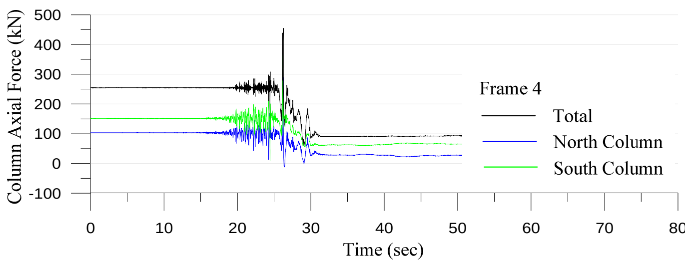

Figure 6. Deterioration of vertical load carrying capacity of Frame 4 during the tests.

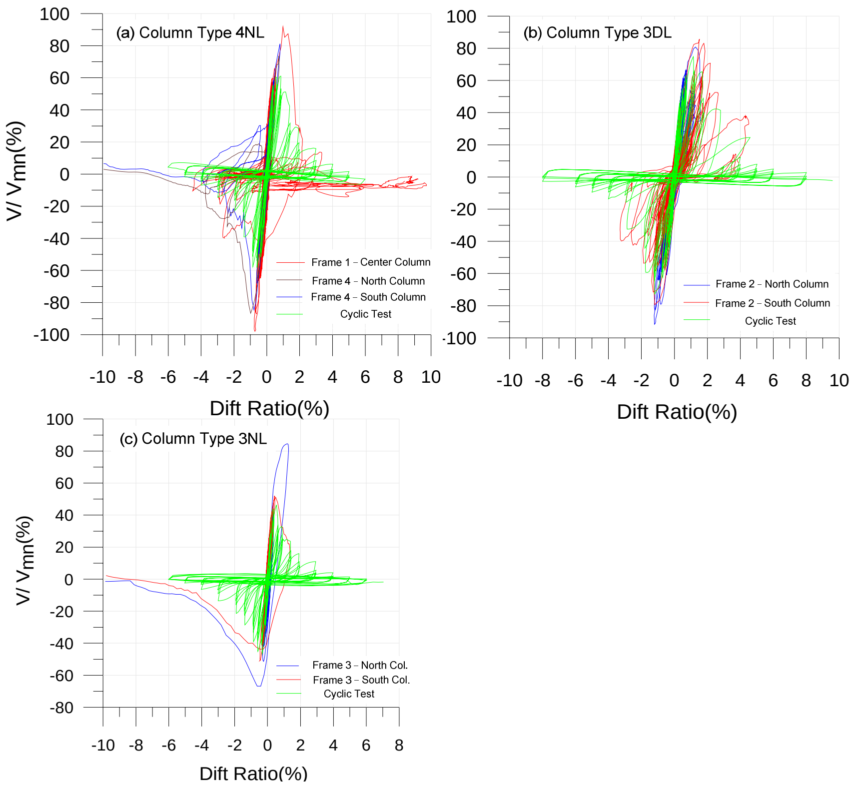

Figure 7. Comparison of hysteretic responses from shaking table tests and static cyclic tests.

To facilitate comparison of shaking table test results with companion cyclic tests, the experimentally obtained peak shear strengths of identical column design are normalized with respect to the flexure-related lateral strength V_{mn}, which was calculated at a maximum concrete strain of 0.003 from monotonic moment-curvature analysis using properties measured during material coupon tests and divided by half the clear column length without taking account of P-Δ effects. The ratio of shear capacity to shear demand reveals information on expected column failure mechanism. Comparison of structural hysteretic data is then made in Fig. 7. The hysteretic responses shown in Fig. 7a were recorded from columns classified as Type 4NL (Table 1) from Frames 1 and 4. The V_{test}/V_{mn} ratios for shaking table tests vary from 83% to 98% even though the columns were of an identical design. The dispersion can be attributed to the inherent spatial variation of concrete strength during construction. The V_{test}/V_{mn} ratio for the full-scale column specimen under reversed cyclic loading is about 60%, which is lower than shaking table tests. The hysteretic responses shown in Fig. 7b were recorded from Type 3DL columns. The V_{test}/V_{mn} ratios for shaking table tests are 82% and 90%, while the full-scale column specimen under reversed cyclic loading is 73%. The hysteretic responses shown in Fig. 7c were from Type 3NL columns. The V_{test}/V_{mn} ratios for shaking table tests are 50% and 85%, while the full-scale column specimen under reversed cyclic loading is 47%. The measured column shear strengths in shaking table tests are higher than those from cyclic test mostly likely due to strain rate effects, while both static and dynamic tests reveal about the same level of drift capacity at shear failure. In addition, the measured shear strengths of columns with nonductile detailing have a larger coefficient of variation that likely resulted from unreliable confining effects of 90°-hook transverse ties. Such non-seismic steel hooks may open up prior to tensile yielding during severe earthquake loadings.

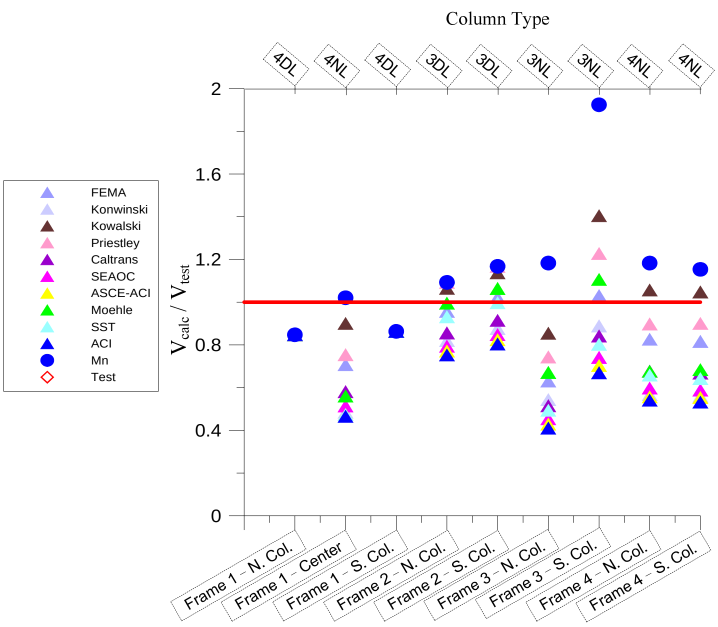

Figure 8. Ratio of calculated shear strength as per assessment models to measured value.

4. COMPARISON WITH ASSESSMENT MODELS

The accuracy of existing shear strength prediction models available from the literature [e.g., ACI 318, AIJ, ASCE/ACI 426, etc.] are evaluated herein using experimental data and the results are shown in Fig. 8, in which the predicted value is normalized with respect to the measured shear strength, and the ratios obtained of nine single columns are presented in the figure. Generally speaking, Kowalski et al. (1997) yields better estimates on the average in most cases with a coefficient of variation of 15%, but unfortunately may overestimate shear strengths in some cases. ACI 318 underestimates column shear strengths at least by 20%, and has a bit higher coefficient of variation (44%). Nonetheless, ACI 318 still produces satisfactory estimates for short columns with ductile detailing. The predictive models available from the literature are inclined to underestimate the actual shear strengths of columns, which is especially true for columns with nonductile detailing.

The experimental hysteretic data is also compared with current assessment models, i.e., ASCE/SEI 41-06, Elwood et al. (2007), Elwood and Moehle (2006), and Zhu et al. (2007), for predicting load deformation curves as shown in Fig. 9, in which the backbone curves calculated by Elwood and Moehle (2006) and Zhu et al. (2007) are for flexure-shear columns as pure shear failure is not considered in their models. Although ASCE/SEI 41-06 (2007) does not provide predictive backbone for pure-shear failure, its update document prepared by Elwood et al. (2007) does additionally include this particular failure type in a descriptive manner. The authors construct the backbone curve according to the update document and fill the missing information using personal judgment and experience. The ASCE/SEI 41-06 backbones in Fig. 9 prove conservative as its suggested post-peak deformation capacity is almost negligible. Although ASCE/SEI 41-06 update procedure is on the safe side from the standpoint of engineering application, future modifications on its predictive curves may still be favorable in order to avoid excessive overdesign in the future. Finally, test results presented in this study are very helpful to subsequent numerical studies in developing advanced nonlinear methods for simulating pure shear failure.

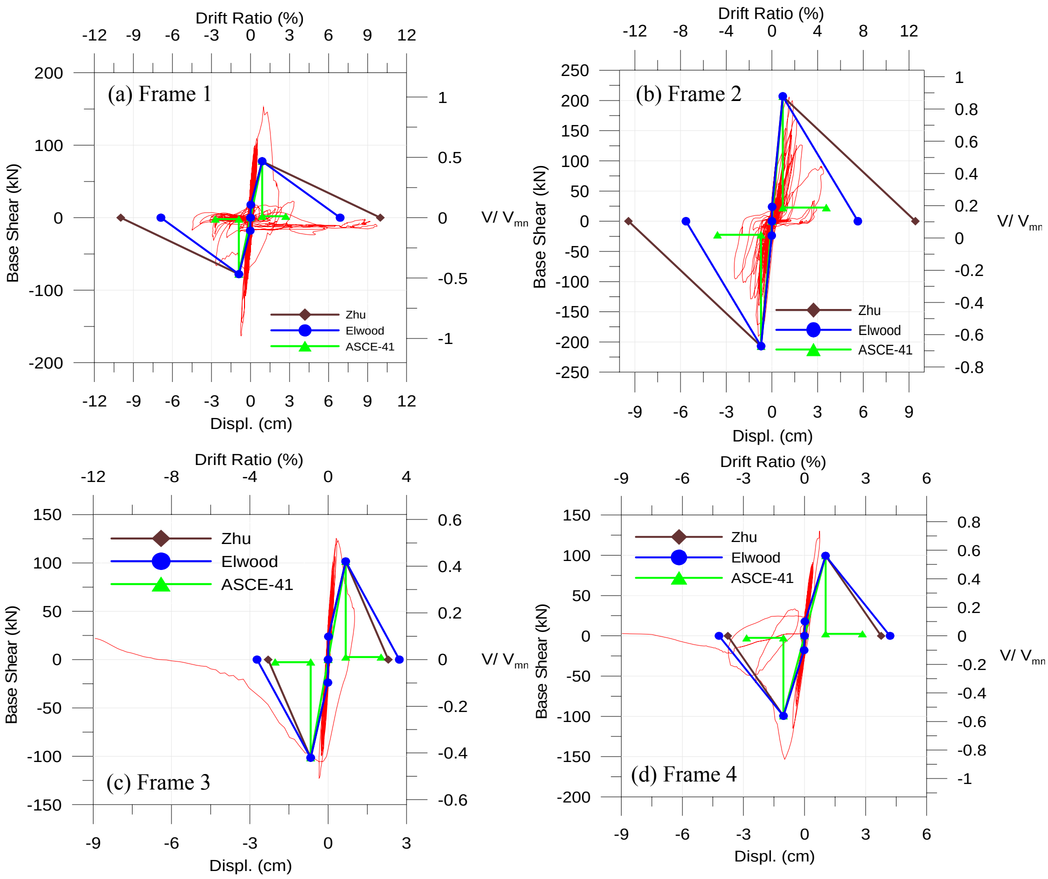

Figure 9. Comparison of existing assessment models with experimental hysteresis of individual columns (results from Zhu *et al.* correspond to the 50th percentile).

5. CONCLUSIONS

This study finds that shear strengths of columns from dynamic tests are higher than those from cyclic tests, which likely comes from strain rate effects. The existing predictive models tend to underestimate the actual shear strengths of columns, which is especially true for columns with nonductile detailing. In addition, ASCE/SEI 41-06 backbone model for short columns proves conservative as its post-peak deformation capacity is almost negligible. Finally, test results presented in this study are very helpful to subsequent numerical studies in developing advanced nonlinear methods for simulating pure shear failure.

REFERENCES

ACI 318 (2008). Building Code Requirements for Structural Concrete (ACI 318-08) and Commentary (ACI 318R-08), American Concrete Institute, Farmington Hills, USA.

AIJ (1994). Structural design guidelines for reinforced concrete buildings, Architectural Institute of Japan.

ASCE/SEI 41-06 (2007). Seismic rehabilitation of existing buildings, America Society of Civil Engineers, Reston, V.A., USA.

ASCE-ACI Committee 426 (1973). Shear strength of reinforced concrete members. ACI 426R-74, Reapproved 1980, Chapters 1 to 4, Proceeding, *ASCE*, **99:ST6**, 1148-1157.

Aschheim, M., and Moehle J.P. (1992). Shear strength and deformability of reinforced concrete bridge columns subjected to inelastic cyclic displacement, Report No.UCB/EERC-92/04, Earthquake Engineering Research Center, University of California at Berkeley, USA.

CALTRANS (1995). Bridge Design Specification, California Department of Transportation, USA.

Elwood, K.J., Matamoros, A.B., Wallace, J.W., Lehman, D.E., Heintz, J.A., Mitchell, A.D., Moore, M.A., Valley, M.T., Lowes, L.N., Comartin, C.D., and Moehle J.P. (2007). Update to ASCE/SEI 41 concrete provisions. *Earthquake Spectra*, **23:3**, 493-523.

Elwood, K.J. and Moehle, J.P. (2006). Idealized backbone model for existing reinforced concrete columns and comparisons with FEMA 356 criteria. *Structural Design of Tall and Special Buildings*, **15**, 553-569.

FEMA 273 (1997). NEHRP Guidelines for the Seismic Rehabilitation of Buildings, Prepared with FEMA funding by ATC and ASCE for the Building Seismic Safety Council, Washington DC, USA.

Hwang S.J. and Lee, H.J. (2002). Strength prediction for discontinuity regions by softened strut-and-tie model. *ASCE Journal of Structural Engineering*, **128:12**, 1519-1526.

Konwinski, C.M. (1996). Shear strength of reinforced concrete bridge piers subject to earthquake loading, M.S. Thesis, Purdue University, USA.

Konwinski, C., Ramirez, J.A., and Sozen M.A. (1995). Shear strength of reinforced concrete columns subject to seismic loading. *Proceedings of the National Seismic Conference on Bridges and Highways: Progress in Research and Practice*, San Diego, California, USA.

Kowalski, M.J., McDaniel, C.C., Benzoni, G., and Priestley, M.J.N. (1997). An improved analytical model for shear strength of circular RC columns in seismic regions, Structural Systems Research Project, University of California, San Diego, USA.

Priestley, M.J.N., Verma, R., and Xiao, Y. (1994). Seismic shear strength of reinforced concrete columns. *ASCE Journal of Structural Engineering*, **120:8**, 2310-2329.

SEAOC (1973). Recommended Lateral Force Requirements and Commentary, Structural Engineers Association of California, Los Angeles, California, USA.

Zhu, L., Elwood, K.J., and Haukaas, T. (2007). Classification and seismic safety evaluation of existing reinforced concrete columns. *ASCE Journal of Structural Engineering*, **133:9**, 1316-1330.